www.dergipark.gov.tr
ISSN:2148-3736
El-Cezerî Fen ve Mühendislik Dergisi
Cilt: 8, No: 1, 2021 (220-230)

El-Cezerî Journal of Science and Engineering
Vol: 8, No: 1, 2021 (220-230)
DOI:10.31202/ecjse.822124

ECJSE

Research Paper / Makale

Understanding the Mechanisms of Adhesion on Model Biomimetic Nanostructures

Taner E. DIRAMA[1a]

Neopol Global A.Ş., Araştırma ve Geliştirme Departmanı, İstanbul, Türkiye
taner.dirama@neopolglobal.com

Received/Geliş: 05.11.2020 **Accepted/Kabul:** 15.01.2021

Abstract: This work investigated the basic adhesion mechanisms of biomimetic elastomeric nanostructures using molecular dynamics simulation. The model based on a network of beads in the form of a specifically shaped pillar interacting with a flat substrate has captured the directionality of adhesion and the geometric asymmetry. The simulation results showed an excellent match with the experimental results of similar systems. Our results have explained the mechanisms behind strong adhesion and easy detachment. The stress concentration occurring when the displacement is imposed in the opposite direction to the angle of pillar tilt allows easy detachment as an unzipping effect. We have also found that by switching the angle of displacement one can increase or decrease the overall adhesion strength 4-folds or more. This work has potential implications for creating uniquely designed micro or nano-structures with desired attachment and detachment properties.

Keywords: biomimetic nanostructure, adhesion, molecular dynamics simulations

Model Biyomimetik Nanoyapılarda Yapışma Mekanizmalarını Anlamak

Öz: Bu çalışma, biyomimetik elastomerik nanoyapıların temel yapışma mekanizmalarını moleküler dinamik simülasyon metodunu kullanarak araştırdı. Düz bir alt tabaka ile etkileşime giren şekillendirilmiş sütun şeklindeki boncuk ağı olarak tasarlanmış bu model, yapışmanın yönselliği ve geometrik asimetri özelliklerini oluşturabildiğini göstermiştir. Simülasyon sonuçları benzer sistemlerin deneysel sonuçlarıyla mükemmel bir uyum göstermiştir. Sonuçlarımız, güçlü yapışma ve kolay ayrılmanın altındaki mekanizmaları açıklayabilmiştir. Yer değiştirme, sütun eğiminin açısına zıt yönde uygulandığında ortaya çıkan gerilme konsantrasyonu, bir fermuar açma etkisi göstererek kolay ayrılmayı sağladı. Ayrıca yer değiştirme açısının farklılaştırılmasıyla genel yapışma mukavemetinin 4 kat veya daha fazla artırılabileceğini veya azaltılabileceğini gözlemledik. Bu çalışmanın, istenen yapışma ve ayrılma özelliklerine sahip benzersiz bir şekilde tasarlanmış mikro veya nanoyapılar oluşturabilme üzerinde potansiyel etkileri bulunmaktadır.

Anahtar Kelimeler: biyomimetik nanoyapılar, yapışma, moleküler dinamik simülasyonları

1. Introduction

Geckos have an exceptional ability to climb a variety of surfaces. The mechanism of strong adhesion is actually a result of the microstructure of geckos' pads. The gecko pads have a hierarchy of structures: rows of ~100 μm long setae branching into hundreds of projections terminating in nanoscale spatula-shaped structures.[1] Microscopy has revealed a spectacular hierarchical structure of gecko's foot with hundreds of setae (i.e. hair) made of keratin. Each setae with 30-130 μm length is consisted of hundreds of projections. These projections or so called spatulae varies from 200 to 500 nm in size.[2] The hierarchical structure creates a remarkable surface coverage accessible to the geckos' pads on the surfaces they climb. Even though the basic interactions between the pads and

How to cite this article
Dirama, T., "Understanding the Mechanisms of Adhesion on Model Biomimetic Nanostructures", El-CezerîJournal of Science and Engineering, 2021, 8(1); 220-230.

Bu makaleye atıf yapmak için
Dırama, T, "Model Biyomimetik Nanoyapılarda Yapışma Mekanizmalarını Anlamak" El-Cezerî Fen ve Mühendislik Dergisi 2021, 8(1); 220-230.
ORCID ID: [a]0000-0003-1975-6505

the surfaces are known to be weak non-bonded van der Waals interactions[3], the large surface area allows the weak interactions to be able to sustain their body weight. These observations have led to several studies to achieve strong adhesion by biomimetic microfiber arrays [4–8]. Experiments have shown that the tilted pillar structure is an effective biologically inspired surface engineering approach to realize strong adhesion.[6]

It is equally remarkable that, besides the strong adhesion, geckos can switch between strong adhesion and easy detachment with minimal effort. Understanding the mechanical principles of this phenomenon and unique geometry in the nanoscale of candidate structures are key components of developing bio-inspired reversible dry adhesives. There have been several research studies creating synthetic pillar structures at micro and nano scale mimicking the hierarchical microstructure of the gecko's foot.[8] These studies have established that several material parameters impact the adhesion behavior of synthetic pillar microstructures. They include fiber aspect ratio, fiber stiffness, shape of the fiber terminal, and tilting of fibers. It has been shown that unlike in the typical wet adhesive surfaces, the geckos pads contain stiff keratinous fibers that form very effective adhesive surfaces.[8] Synthetic structures made of less stiff fibers run into clumping of fibers, which significantly deteriorates the adhesive behavior.[9] The tilting of the fibers has been demonstrated to create adhesive anisotropy via friction experiments on a surface made of fibrillar microstructural arrays.[4]

The fabrication of bio-mimetic microstructures include a common method of polymer replica molding[10] and recently emerging techniques of nano-imprint lithography[11] and colloidal lithography[12]. Regardless of the fabrication method, creating irregular and unique shapes at the nanoscale in a hierarchical structure is a very challenging task.[8] On the other hand, theoretical or computational modeling are ideal methods to investigate this phenomenon, since they allow creating nanoscale geometries while capturing the fundamental van der Waals interactions.

The molecular modeling of structures mimicking the unique shape of a spatula approximated as soft networked systems are achievable. There have been several computational modeling studies modeling crosslinked polymers that can be used as material for this purpose. Previously, a single step cross-linking structure of epoxy resin was modeled[13] and a poly(dimethyl siloxane)) (PDMS) network was modeled by carrying out crosslinking in a dynamic fashion[14]. These atomistic models captured atomistic resolution of these system, at the expense of limited scale. An alternative approach used a coarse grained representation of these networks with a dynamical cross-linking procedure [15–18]. Recently, a theoretical model of a fiber array with hierarchical structure was presented.[19] This model has taken both the seta and the terminal spatula in gecko's pads. The authors were able to predict the adhesive force of the system with good a good match with observations in the nature. Another recent study used a coarse-grained model to investigate the mechanical properties of gecko setae and spatula[20]. The model considered soft and stiff material types corresponding to the proximal and distal regions, respectively. The study has demonstrated the anisotropic behavior by comparison of the shear and Young's modulus of the stiff fibril region.

The main objective of this work is to understand the mechanisms behind the adhesion of bio-inspired nanostructures. We also wanted to shed some light on related phenomena such as the directionality of adhesion, the geometric asymmetry, strong adhesion and easy detachment using a computational model. Such understanding can help understand design parameters and guide relevant material fabrication efforts.

In Sec. 2, we explain the details of the model used in building the model system and the simulation protocol. In Sec. 3, we provide insight into the results of our simulations and we share our concluding remarks in Sec. 4.

2. Modeling and Simulation Method

A 2-dimensional cross-section of a spatula is shown in Figure 1. We simplified this structure to a parallelogram pillar. Since it is important to capture the geometric asymmetry in our model, the pillars are tilted with respect to the surface normal. The pillar structure was modeled using cross-linked beads using bead-spring model [15–17]. The interactions were represented using 6-12 Lennard-Jones (LJ) potential.

$$U_{LJ}(r) = 4u_0\left[\left(\frac{d}{r}\right)^{12} - \left(\frac{d}{r}\right)^{6}\right] \quad (1)$$

u_0 is the LJ energy, d is the LJ diameter and r is the distance between a given pair of beads. Cutoff distance was set at 2.5 d. u_0 and d are taken as being equal to 1.

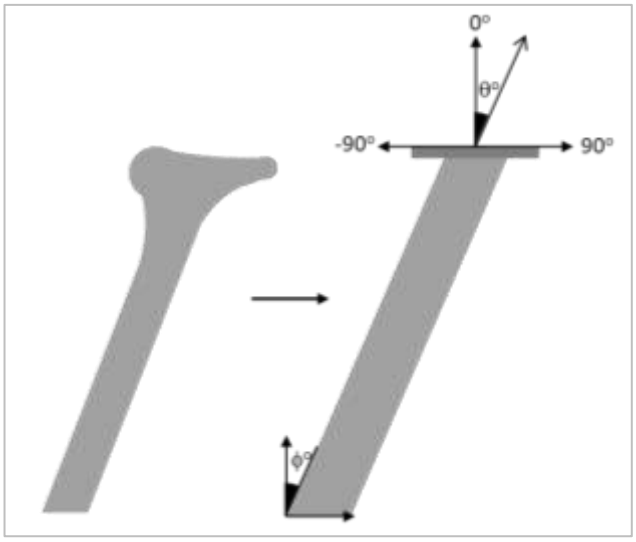

Figure 1. Schematic diagram of spatula on the left. A simplified tilted pillar and substrate surface model with displacement and tilt angles is shown on the right.

The bonds were represented a quartic bond potential. It is has been previously used in modeling of similar systems[15]

$$U_q(r) = \begin{cases} k(y-b_1)(y-b_2)y^2 + U_0, & r < r_c \\ U_0, & r > r_c \end{cases} \quad (2)$$

where $k = 1434.3\ u_0/d^4$, $y = r - \Delta r$, $b_1 = -0.759$ d, $b_2 = 0$, $\Delta r = r_c = 1.5$ d and $U_0 = 67.223\ u_0$. r_c is the cutoff distance. The bond potential is turned off at distances larger than r_c. Once bonds form they become permanent. The ceiling of the bonding force is $156.7\ u_0/d$. This force is 65 times that of the LJ force = $2.4\ u_0/d$.

Large-scale Atomic/Molecular Massively Parallel Simulator (LAMMPS) program was used for the simulations [21]. The Verlet algorithm [22] with a time step of 0.05 τ (τ = LJ time unit). Nose-Hoover algorithm was used to control pressure and temperature (damping constant was set at 0.1τ). The crosslinking simulations initiated two and three beads trapped inside temporary two layers of beads organized and fixed in space (i.e., a contour layer) according to the geometry of the pillar desired. The bead chains had one crosslinking bead for the following the of crosslinking process. These crosslinking beads interact with all beads with the exception of the same kind of beads. A total of 37,585 beads were used. The ratio precursors with different lengths (2 or 3 beads) were decided according to the stoichiometry required. The box was initially equilibrated in a constant

volume and temperature (i.e., NVT) ensemble at reduced temperature unit (T^*) =1. After that, the equilibration was performed in a constant pressure and temperature (i.e., NPT) ensemble to reach the density at the equilibrium.

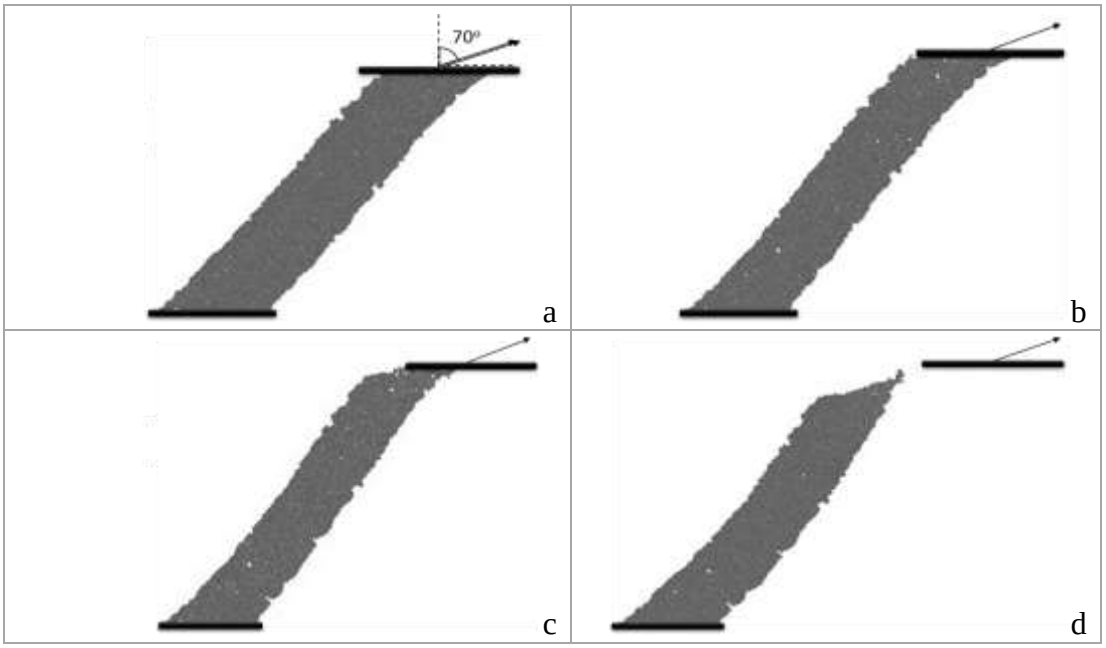

Figure 2. Visualizations of the displacement simulations for a pillar of tilt angle, $\phi = 40^o$ and separation angle, $\theta = 70^o$ at various stages of detachment.

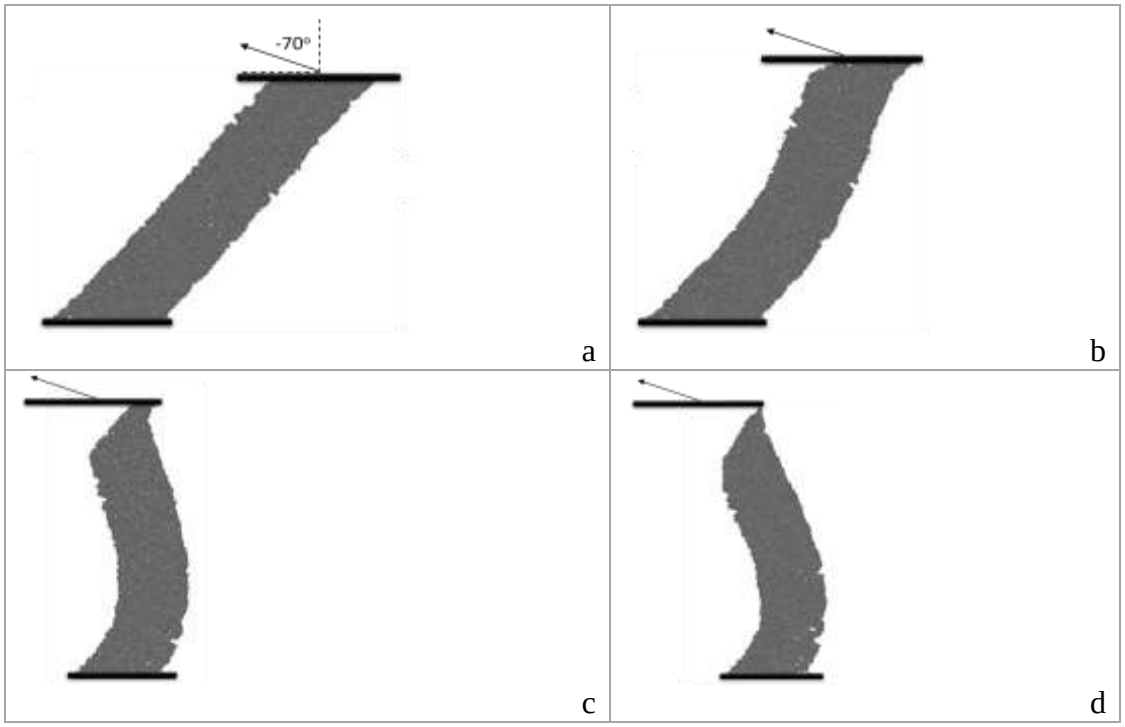

Figure 3. Visualizations of the displacement simulations for a pillar of tilt angle, $\phi = 40^o$ and separation angle, $\theta = -70^o$ at various stages of detachment.

Subsequent to equilibration of the mixture, dynamical crosslinking was performed within the body of the mixture and also to the bottom layer of 509 beads. The bottom layer was used to fixate the structure to this fixed layer of beads. The beads of the fixed layer were made of (111) plane of FCC

lattice structure. The lattice spacing was set at 1.2. The bead pairs as candidates for crosslinking distance-based method was used. Pairs with distances starting from 1.1 *d* until 1.35 *d* were cross-linked. The cross-linking of the cross-linkers to beads was done iteratively. In each iteration; pairs were determined, bonds were formed, and the system was equilibrated. As a result, 43,398 crosslinking bonds were created. The network was equilibrated at $T^* = 1$. The bond forces were calculated using quartic potential. The system was slowly cooled down to 0.3 T^*.

After creating an intact pillar structure with a rubber-like material, we placed a layer of substrate beads on top of the pillar as in Figure 2. The substrate beads were made of (111) plane of FCC lattice structures with a lattice spacing of 1.2. This layer was brought on the pillar surface and a further equilibration simulation run of 100,000 steps was performed. This substrate layer was displaced in the direction defined by the separation angle (θ) in simulations that were run for 200,000 steps at a displacement speed of $0.5\times10^{-1}d/\tau$.

We created pillars at 7 different tilt angles (ϕ) starting from 0^o to 60^o at 10^o increments to investigate the effect of the tilt angle. For each of the pillars, we ran simulations of 19 different separation angles (θ) from -90^o to 90^o at 10^o increments. The visualizations of the displacement simulations for a pillar of the tilt angle, $\phi = 40^o$, and the separation angle, $\theta = 70^o$ and -70^o are shown in Figure 2 and Figure 3, respectively. The main variables and parameters used in the model were listed in Table 1.

Table 1. Parameters and variables used in the model.

Parameter /Variable	Description	Set Value
$\mathbf{U_{LJ}}$	Energy between pairs per 6-12 Lennard-Jones Potential	-
$\mathbf{u_0}$	Lennard-Jones energy in 6-12 Lennard-Jones Potential	-
d	Lennard-Jones diameter	-
r	Distance between two pairs	-
$\mathbf{U_q}$	Bond energy per Quartic Bond Potential	-
k	Quartic Bond Potential Constant	$1434.3\ u_0/d^4$
r	Bond length in Quartic Bond Potential	-
$\mathbf{r_c}$, $\Delta\mathbf{r}$	Cutoff length in Quartic Bond Potential	1.5 d
y	Deviation of the bond length from the bond length in Quartic Bond Potential	$r - \Delta r$
$\mathbf{U_0}$	Cutoff length in Quartic Bond Potential	$67.223\ u_0$
$\mathbf{b_1}$	A constant in Quartic Bond Potential	-0.759 d
$\mathbf{b_2}$	A constant in Quartic Bond Potential	0
$\mathbf{T^*}$	Reduced temperature unit	-
τ	Lennard-Jones Potential time unit	-
ϕ	Tilt angles of the pillar	-
θ	Angle of separation	-

3. Results and Discussion

The aspect ratio of the pillar is one of the important design parameters in a synthetically created bio-mimetic surface.[8] In pillars made of soft materials such as PDMS, a long aspect ratio causes clumping[9] which reduces the adhesion strength. On the other hand, for rigid fibers such as carbon nanotubes[23], the desired adhesive strength can only achieved via high aspect ratio. Our choice of the aspect ratio (= 3.1) was based on these two design criteria. This selection was supported by

earlier studies, where the gecko's adhesion mechanism was successfully demonstrated using a synthetically fabricated polymeric microstructures [2,6].

The force exerted to the substrate layer by its interaction with the pillar as it was being separated was calculated in the lateral (F_x) and the vertical (F_y) directions. The unit of force is u_0/d (u_0 is the LJ energy, d is the LJ diameter). The interactions between the substrate and the pillar are non-bonded van der Waals interactions. F_x as a function of the simulation time (t) was presented in Figure 4. $F_x(t)$ was at its maximum when the substrate layer was in direct contact with the top surface of the pillar. Shortly after the F_x begins to decay rapidly as a sign of rapid detachment of the pillar from the surface. At t=500 it decays entirely.

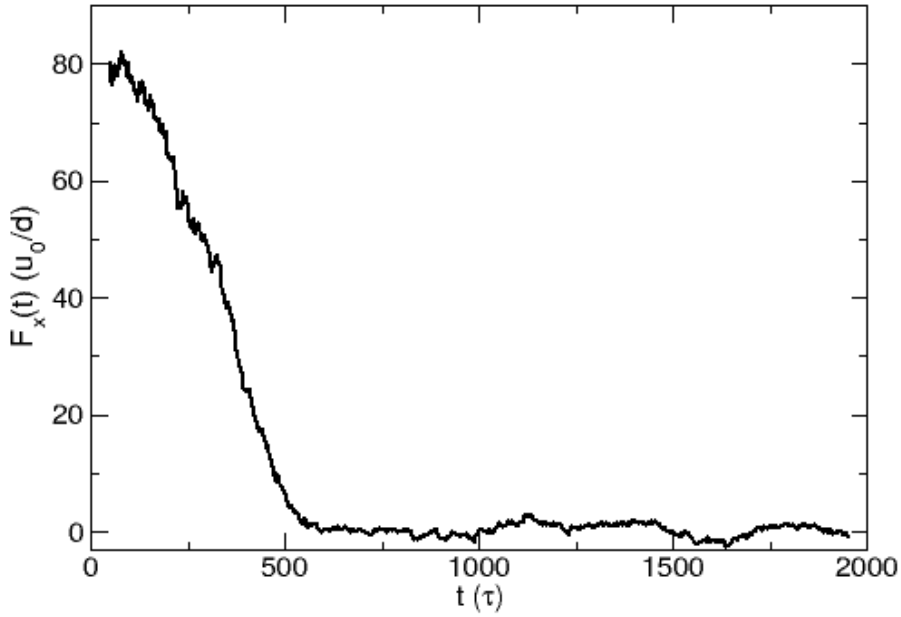

Figure 4. Lateral force (F_x) as a function of simulation time (t) for a pillar with $\phi = 20^o$.

By varying tilt angles (ϕ) and separation angles (θ), we carried out a total of 133 simulations to generate data that allows us to investigate the directionality of adhesion. In Figure 5, we present F_x as a function of the separation angle θ for each pillar with the tilting angle ϕ. Each data point was derived from the same type of graph as shown in Figure 4 at maximum $F_x(t)$. At $\phi = 0^o$, when there was no tilt, F_x exhibited a bell-shaped dependence on θ. F_x was minimum at $\theta = 0^o$ and increases symmetrically going away from it. This was expected behavior, since lifting the straight pillar does not involve any lateral forces. As the direction of the displacement changed, the lateral forces appeared and reached a maximum at -90^o and 90^o pulls. The center of the bell-shaped curve moved towards the opposite of the tilting angle ϕ, when the same simulations were performed on tilted pillars.

When we analyze the vertical component of the force vector F_y, at $\phi = 0^o$ in Figure 6, the maximum resistance to the separation occurred at $\theta = 0^o$, when the substrate was pulled vertically. F_y shows an upside-down bell-shaped curve dependence on the displacement angle θ. As the tilting angle ϕ increases, the center of the curve F_y shifted towards the opposite direction of the tilting angle. At $\phi = 30^o$ and higher, the peak point diminished and at $\phi = 50^o$ the F_y showed a gradual increase as a function of displacement angle θ from -90^o to 90^o.

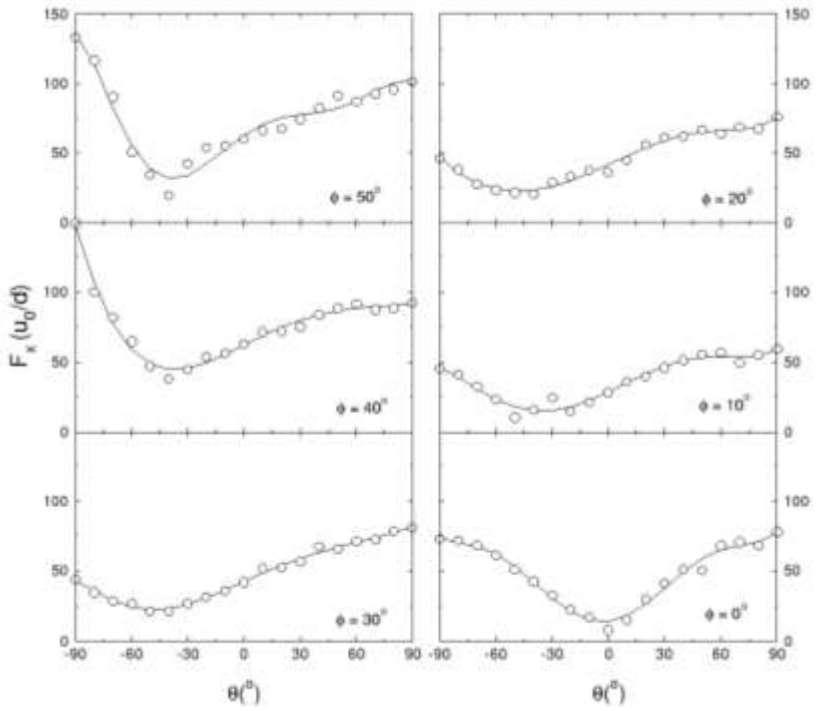

Figure 5. The lateral component of the detachment force (F_x) vs. the displacement angle θ for pillars with tilt angles (ϕ) 0^o to 50^o with increments of 10^o. Open circles are the data points. The lines are the polynomial fits to the data.

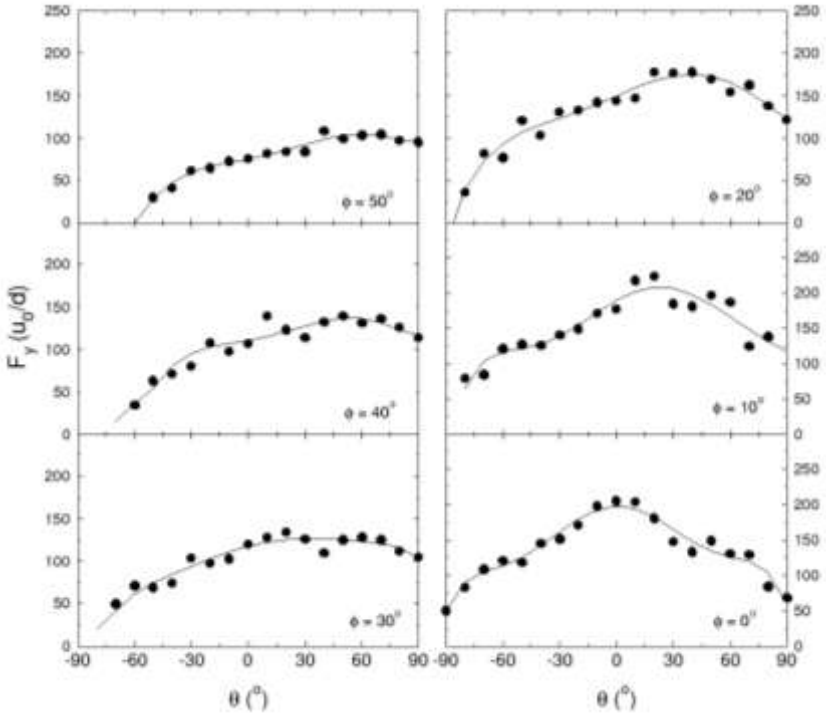

Figure 6. The vertical component of the detachment force (F_y) vs. the displacement angle θ for pillars with tilt angles (ϕ) 0^o to 50^o with increments of 10^o. Closed circles are the data points. The lines are the polynomial fits to the data.

There are several important inferences we can draw from Figure 5 and Figure 6. First of all, these graphs demonstrate that the model is able to capture the directionality of adhesion for the pillar with

no tilting. In other words, the resistance to separation in both lateral and vertical directions are dependent on the angle of the displacement. This is an important outcome of our simulations because it gives us confidence in our model to capture the basic mechanism of non-bonded adhesion of soft material on to a rigid substrate. In addition, we observe the geometric asymmetry: the tilting of the pillar results in significant changes in adhesion strength in both lateral and vertical components. We discuss the potential implications of these results later in the article.

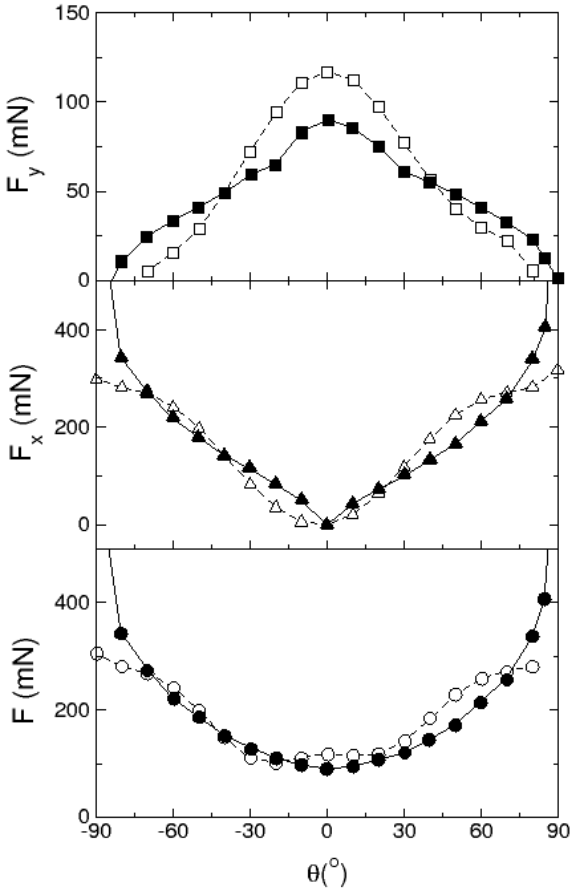

Figure 7. The detachment forces in the vertical (F_y) (top), lateral (F_x) (middle) directions, and the total force (F) (bottom) for the pillar with no tilt ($\phi = 0^o$). Open symbols are the simulation results and closed symbols are the experimental results[6]. The simulation results of F_x and F_y have been linearly scaled to match their arbitrary dimension to the dimensions of the experimental results.

Having established that the model is able to capture previously reported basic adhesion mechanisms of a nano pillar – rigid substrate system, we would like to compare the adhesion behavior of our models to experimental results of similar systems [6]. The resistance to separation in the lateral (F_x), the vertical (F_y) directions, and the total force (F) for pillars with no tilt are presented in Figure 7. There is a remarkable overlap of the experimental results to our models in the total force and its vectoral components. The only qualitative difference observed is that our models show a steeper peak in F_y compared to the experimental results. This is possibly due to the fact that the dimensions of the pillar in our model is in the nano-scale versus the experiments that were carried out on micron-sized pillars. This difference in scale might very well have resulted in a steeper response of the vertical component of the separation force compared to the experiments.

A notable comparison is also observed for the pillar with a 40^o tilt between the experimental and the modeling results as shown in Figure 8. The vertical component of the detachment force overlaps very nicely over the entire range of displacement directions. For the lateral force component, just as

in the experimental results, the simulation results also predict the shifting of the bottom of the curve away from the angle of the tilt direction. However, the experiment shows this valley at around -20^o versus -35^o in the simulations. One possible explanation for this shift is that the tilt angle of the pillars' changes during the adhesion experiments.[6] This might have played a role in the difference in the results.

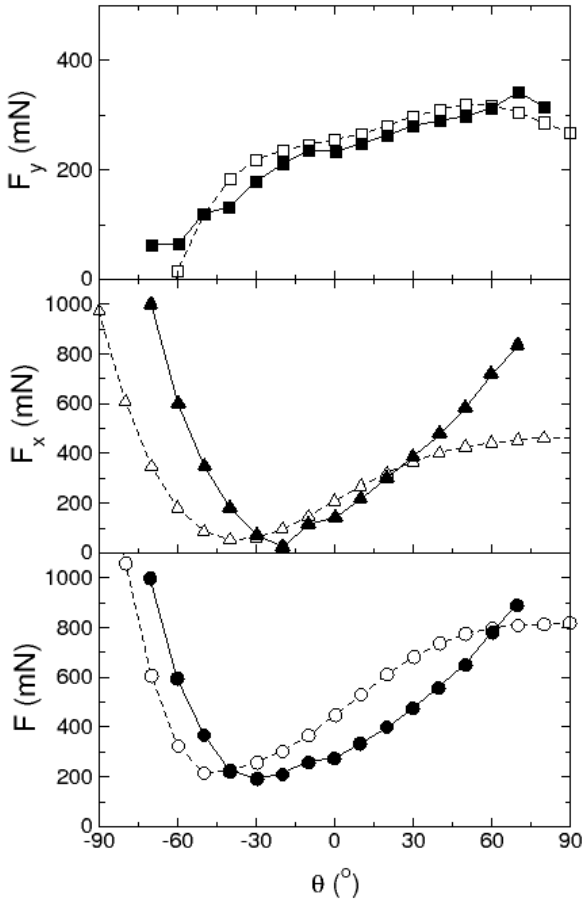

Figure 8. The detachment forces in the vertical (F_y) (top), lateral (F_x) (middle) directions, and the total force (F) (bottom) for the pillar with no tilt ($\phi = 40^o$). Open symbols are the simulation results and closed symbols are the experimental results[6]. The simulation results of F_x and F_y have been linearly scaled to match their arbitrary dimension to the dimensions of the experimental results.

Both experimental and simulation results show that the vertical detachment force (F_y) is small at low displacement angles and steadily increases as a function of θ, while the lateral detachment force (F_x) exhibits a non-centric quadratic function. It is worth highlighting that at the displacement angle θ, where the minimum lateral detachment force (F_x) occurs, there is substantial vertical detachment force (F_y). This means that when the pillar can be moved laterally with almost no resistance, the pillar still adheres to the substrate with considerable adhesive strength.

The total detachment force curve shows how one could manipulate the angle of displacement to switch between easy detachment and strong adhesion. For example, there is a 4-fold increase in the detachment force from about 200 mN to 800 mN by switching the displacement angle from -50^o to 80^o. The difference between the detachment mechanisms at these two displacement angles can be visualized in Figure 2 and Figure 3. When the angle of displacement is in the same direction as the tilt angle of the pillar the detachment mechanism between the pillar and the substrate is similar to a

uniaxial pull (Figure 2). On the other hand, when the angle of displacement is in the opposite direction to the angle of tilt, then the detachment mechanism is similar to a peeling action (Figure 3). The peeling mechanism allows the stress imposed by displacing the substrate from the pillar to concentrate at a small area. The stress concentration in this area allows layers to begin to detach at smaller overall detachment forces and continue throughout the area of contact until complete separation occurs. This mechanism, we call it unzipping, is the underlying explanation of the geometric asymmetry.

4. Conclusion

In this study, we devised a relatively simple model of an elastomeric nanostructure with geometries that allowed us to investigate basic adhesion mechanisms. The results of the molecular dynamics simulations have shown an excellent match with the experimental results of similar systems. Our model has captured several important mechanisms of adhesion: the directionality of adhesion, the geometric asymmetry, strong adhesion and, easy detachment. We have found that one can increase or decrease the overall adhesion strength 4-folds or more by changing the angle of displacement. This work has potential implications for creating uniquely designed micro or nano-structures with desired attachment and detachment properties.

References

[1]. Krause DW. "Functional Vertebrate Morphology. Milton Hildebrand, Dennis M. Bramble , Karel F. Liem , David B. Wake". Q Rev Biol, 1986, 61 (2): 280–1.
[2]. Gao H, Wang X, Yao H, Gorb S, Arzt E. "Mechanics of hierarchical adhesion structures of geckos". Mech Mater, 2005, 37 (2): 275–85.
[3]. Autumn K, Liang YA, Hsieh ST, Zesch W, Chan WP, Kenny TW, et al. "Adhesive force of a single gecko foot-hair". Nature, 2000, 405 (6787): 681–5.
[4]. Lee J, Fearing RS, Komvopoulos K. "Directional adhesion of gecko-inspired angled microfiber arrays". Appl Phys Lett, 2008, 93 (19): 191910.
[5]. Kamperman M, Kroner E, Campo A del, McMeeking RM, Arzt E. "Functional Adhesive Surfaces with “Gecko” Effect: The Concept of Contact Splitting". Adv Eng Mater, 2010, 12 (5): 335–48.
[6]. Yao H, Rocca GD, Guduru P r, Gao H. "Adhesion and sliding response of a biologically inspired fibrillar surface: experimental observations". J R Soc Interface, 2008, 5 (24): 723–33.
[7]. Schubert BE, Gillies AG, Fearing RS. "Angled microfiber arrays as low-modulus, low Poisson\textquotesingles ratio compliant substrates". J Micromechanics Microengineering, 2014, 24 (6): 065016.
[8]. Brodoceanu D, Bauer CT, Kroner E, Arzt E, Kraus T. "Hierarchical bioinspired adhesive surfaces—a review". Bioinspir Biomim, 2016, 11 (5): 051001.
[9]. Spolenak R, Gorb S, Arzt E. "Adhesion design maps for bio-inspired attachment systems". Acta Biomater, 2005, 1 (1): 5–13.
[10]. Greiner C, Arzt E, Campo A del. "Hierarchical Gecko-Like Adhesives". Adv Mater, 2009, 21 (4): 479–82.
[11]. Schift H. "Nanoimprint lithography: 2D or not 2D? A review". Appl Phys A, 2015, 121 (2): 415–35.
[12]. Vogel N, Retsch M, Fustin C-A, del Campo A, Jonas U. "Advances in Colloidal Assembly: The Design of Structure and Hierarchy in Two and Three Dimensions". Chem Rev, 2015, 115 (13): 6265–311.
[13]. Yarovsky I, Evans E. "Computer simulation of structure and properties of crosslinked polymers: application to epoxy resins". Polymer, 2002, 43 (3): 963–9.

[14]. Heine DR, Grest GS, Lorenz CD, Tsige M, Stevens MJ. "Atomistic Simulations of End-Linked Poly(dimethylsiloxane) Networks: Structure and Relaxation". Macromolecules, 2004, 37 (10): 3857–64.
[15]. Stevens MJ. "Interfacial Fracture between Highly Cross-Linked Polymer Networks and a Solid Surface: Effect of Interfacial Bond Density". Macromolecules, 2001, 34 (8): 2710–8.
[16]. Tsige M, Lorenz C, Stevens M. "Role of network connectivity on the mechanical properties of highly cross-linked polymers". 2004, .
[17]. Tsige M, Stevens MJ. "Effect of Cross-Linker Functionality on the Adhesion of Highly Cross-Linked Polymer Networks: A Molecular Dynamics Study of Epoxies". Macromolecules, 2004, 37 (2): 630–7.
[18]. Dirama TE, Varshney V, Anderson KL, Shumaker JA, Johnson JA. "Coarse-grained molecular dynamics simulations of ionic polymer networks". Mech Time-Depend Mater, 2008, 12 (3): 205–20.
[19]. Zhang QK, Li LX. "Study on the structural parameters and adhesive force of gecko seta". J Adhes, 2020, 96 (16): 1449–65.
[20]. Endoh KS, Kawakatsu T, Müller-Plathe F. "Coarse-Grained Molecular Simulation Model for Gecko Feet Keratin". J Phys Chem B, 2018, 122 (8): 2203–12.
[21]. Plimpton S. "Fast Parallel Algorithms for Short-Range Molecular Dynamics". J Comput Phys, 1995, 117 (1): 1–19.
[22]. Verlet L. "Computer “Experiments” on Classical Fluids. I. Thermodynamical Properties of Lennard-Jones Molecules". Phys Rev, 1967, 159 (1): 98–103.
[23]. Qu L, Dai L, Stone M, Xia Z, Wang ZL. "Carbon Nanotube Arrays with Strong Shear Binding-On and Easy Normal Lifting-Off". Science, 2008, 322 (5899): 238–42.